Proceedings of SMASIS08
ASME Conference on Smart Materials, Adaptive Structures and Intelligent Systems
October 28-30, 2008, Ellicott City, Maryland, USA

SMASIS2008-605

ENERGY HARVESTING BY PYROELECTRIC EFFECT USING PZT

J. Xie, P. P. Mane, C. W. Green, K. M. Mossi[†]
Department of Mechanical Engineering
Virginia Commonwealth University
Richmond, VA 23284
[†]E-mail: kmmossi@vcu.edu

Kam K. Leang[‡]
Department of Mechanical Engineering
University of Nevada, Reno
Reno, NV 89557
[‡]E-mail: kam@unr.edu

ABSTRACT

This paper considers energy harvesting using pyroelectric materials such as PZT-5A and thin-films. A simple model is used to predict the power generated based on the measured temperature of the material as a function of time. The measured and predicted results are presented and compared. In particular, the measured peak power density for a PZT-5A sample was 0.23 μWcm^{-2} *for a maximum temperature rate of approximately* 15 $^{\circ}Cs^{-1}$. *The predicted peak power density under the same boundary conditions for thin-film lead scandium tantalate was over* 125 μWcm^{-2}. *The power density is shown to be highly dependent upon the surface area and the pyroelectric coefficient, underlining the importance of maximizing these parameters.*

1 INTRODUCTION

Due to recent advances in low-power portable electronics and the fact that batteries in general provide a finite amount of power, attention has been given to explore methods for energy harvesting and scavenging. Energy can be recovered from mechanical vibration [1], light, and spatial and temporal temperature variations [2, 3].

Thermal energy in the environment is a potential source of energy for low-power electronics. For example, a recent commercial product, a wristwatch, uses thermoelectric modules to generate enough power to run the clock's mechanical components [3]. The thermoelectric modules work on the thermal gradient provided by body heat. A recent patent was issued for energy harvesting using novel thermoelectric materials [4], and batteries can be recharged using thermal gradients [5]. Ferromagnetic materials have been exploited to convert thermal into electrical energy [6].

Rather than harvesting energy from spatial temperature gradients, pyroelectric materials produce power from temporal temperature fluctuations [7]. In particular, charge is produced when the material's temperature is altered as a function of time; likewise, a change in temperature results in mechanical deformation. Recent work was presented on using PZT pyroelectric materials for energy harvesting and storage [8–10]. Several factors must be considered to optimize the performance of such materials for a given application. For example, the material's geometry, boundary conditions, and even the circuitry used to harvest power must be carefully considered [11]. In terms of geometry, thicker material may produce high voltages, but the resulting high thermal mass may increase the time it takes to heat and cool the material.

One avenue to enhance energy generation is to use pyroelectric materials with significantly higher pyroelectric coefficients. A recent study showed that thin films with volume fractions similar to bulk PZT exhibit orders of magnitude higher pyroelectric coefficients [12]. The use of pre-stressed materials may also enhance performance [17].

In the following, a simple model is developed to predict the power generated based on the temperature of a pyroelectric material. The model is validated with a PZT-5A sample. Then the model is used to predict power generation for other pyroelectric materials with higher pyroelectric coefficients, such as thin-film lead scandium tantalate [13, 14] and lead magnesium niobate - lead titanate [11, 15].

The paper is organized as follows. Section 2 describes the modeling. Then Section 3 discusses the experimental system, and Section 4 presents the measured and predicted results. Finally, conclusions and acknowledgements are found in Sections 5 and 6, respectively.

2 A SIMPLE MODEL

A material is considered to exhibit the pyroelectric effect when a change in the material's temperature with respect to time (temporal fluctuation) results in the production of electric charge [7,10]. In particular, the detectable current $i_p(t)$ of a pyroelectric material is proportional to the rate of change of its temperature [7], *i.e.*,

$$i_p(t) = p' A \frac{dT(t)}{dt}, \tag{1}$$

where p' is the component of the pyroelectric coefficient vector $\mathbf{p}$ orthogonal to the electrode surface of area A; and $T(t)$ denotes the temperature with respect to time. For convenience, the heating and cooling behavior of the material was not considered in the model.

A lumped-parameter model of a pyroelectric element is shown in Fig. 1. The pyroelectric element was modeled as a current source $i_p(t)$ in parallel with an internal capacitance C_p. The figure also shows the pyroelectric element connected in parallel with an external capacitor C_e and resistor R_e. The objective was to determine the element's output voltage $V_p(t)$ and power $P(t)$ generated for a given temperature profile $T(t)$.

For a given temperature profile $T(t)$, the instantaneous power dissipated by the resistor R_e can be determined by measuring the output voltage $V_p(t)$, *i.e.*,

$$P(t) = \frac{V_p^2(t)}{R_e}. \tag{2}$$

On the other hand, the generated power can be predicted using Eq. (1) as follows. Assuming zero initial conditions, summing currents in the circuit shown in Fig. 1 gives

$$p' A s T(s) = C s V_p(s) + \frac{1}{R_e} V_p(s), \tag{3}$$

where s is the Laplace variable and $T(s)$ and $V_p(s)$ are the Laplace transforms of the temperature and output voltage, respectively. Therefore, the transfer function relating the input temperature $T(s)$ to the output voltage $V_p(s)$ is

$$G(s) \triangleq \frac{V_p(s)}{T(s)} = \frac{p' A s}{C s + 1/R_e}. \tag{4}$$

Finally, the predicted power generation based on a given temperature profile $T(t)$ for the pyroelectric element can be determined by first using Eq. (4) to determine the output voltage $V_p(t)$. Then, the power across the resistor can be calculated using Eq. (2). The thermal dynamic effects such as the heating and cooling rate of the pyroelectric element are not captured in the above expression.

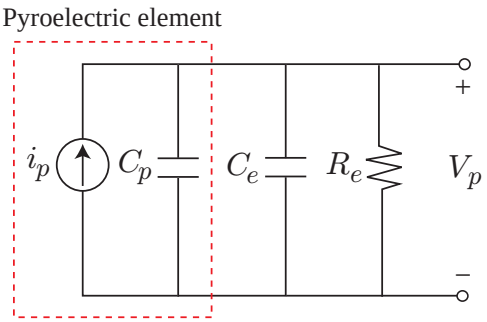

Figure 1. A lumped-parameter model of a pyroelectric element, which is modeled as a current source $i_p(t)$ in parallel with an internal capacitance C_p, connected in parallel to an external capacitor C_e and resistor R_e. The current i_p is proportional to the rate of change of temperature of the device. The voltage generated by the pyroelectric element is denoted by $V_p(t)$.

3 THE EXPERIMENTAL SYSTEM

An experimental system was created to validate the simplified model to predict the power generated for a sample pyroelectric element. The pyroelectric element was PZT-5A, with area $A = 1.44$ cm^2 (1.20 cm $\times$ 1.20 cm), thickness of 150 μm, measured pyroelectric coefficient $p' = 238$ μCm^{-2}K^{-1}, and capacitance $C_p = 45$ nF.

The experimental system is pictured in Fig. 2, where the PZT element was bonded to a thin resistance heater (Minco HK5578 R35.0L12B, 1.91 cm $\times$ 1.91 cm). The heater was used to control the temperature of the pyroelectric element and a Type K thermocouple sensor was attached to the backside of the resistance heater to measure the temperature of the heater. The measured temperature was assumed to be the temperature of the PZT. Also, the thermocouple sensor was passed through an Analog Devices AD595 monolithic thermocouple amplifier and the signal was recorded by a desktop computer with a data acquisition system (National Instruments, LabPC+, 12-bit).

Figure 3(a) shows the block diagram of the temperature control system used to control the temperature of the PZT element. The current amplifier circuit for the resistance heater is shown in Fig. 3(b). Finally, the circuit diagram for measuring the generated voltage to compute the power across the resistor R_e is shown in Fig. 3(c). As an illustrative example, the external capacitance

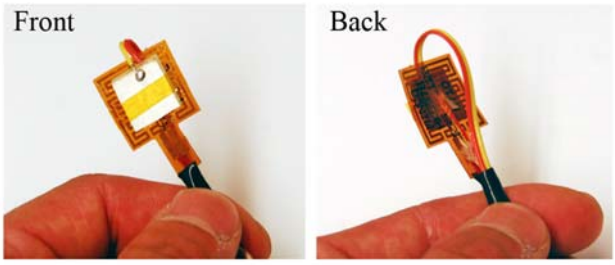

Figure 2. Photographs of front and back view of the PZT-5A sample mounted to a thin-film resistance heater (Minco HK5578 R35.0L12B). The thermocouple temperature sensor is fixed to the backside of the heater.

and resistance were chosen as $C_e = 0$ and $R_e = 1$ MΩ, respectively. The chosen resistor value was not optimized for maximum power generation.

4 THE MEASURED AND PREDICTED RESULTS

The control system was tuned to achieve a relatively-high temperature rate, where the maximum was 15.65 °Cs^{-1} [see dash-line plot in Fig. 4(a)] over a temperature range between 29.79 to 102.78°C. The resulting measured and predicted output voltage V_p for the PZT element are shown in Fig. 4(b). The measured and predicted peak voltages were 0.58 V and 0.53 V, respectively. Both the voltage profile and peak voltage for the measured and predicted results compared well [see Fig. 4(b)]. Finally, the measured and predicted power densities (normalized with area of PZT element) are depicted in Fig. 4(c), where the peak values for the measured and predicted results were 0.23 μWcm^{-2} and 0.20 μWcm^{-2}, respectively. Like the voltage results, the measured and predicted power densities were also in good agreement.

Discrepancies can be attributed to several factors. First, the temperature of the PZT element was measured at a single point using the thermocouple sensor, and thus temperature may not have been uniform across the sample. Second, the temperature was measured on the backside of the resistance heater and was assumed to be the temperature of the PZT element.

To study the potential of using other pyroelectric materials for power generation, the model given by Eq. (4) combined with the measured temperature profile shown in Fig. 4(a) were used to predict power generation. In particular, thin-film lead scandium tantalate (PST) with pyroelectric coefficient p'=6000 μCm^{-2}K^{-1} [13, 14] and lead magnesium niobate - lead titanate (PMN-PT) with $p' = 300$ to over 1000 μCm^{-2}K^{-1} [11, 15] were considered. Likewise, it has been noted that residual stresses in PZT materials can increase the pyroelectric coefficient [16], and therefore such materials are also a good candidate for enhanced power generation [17].

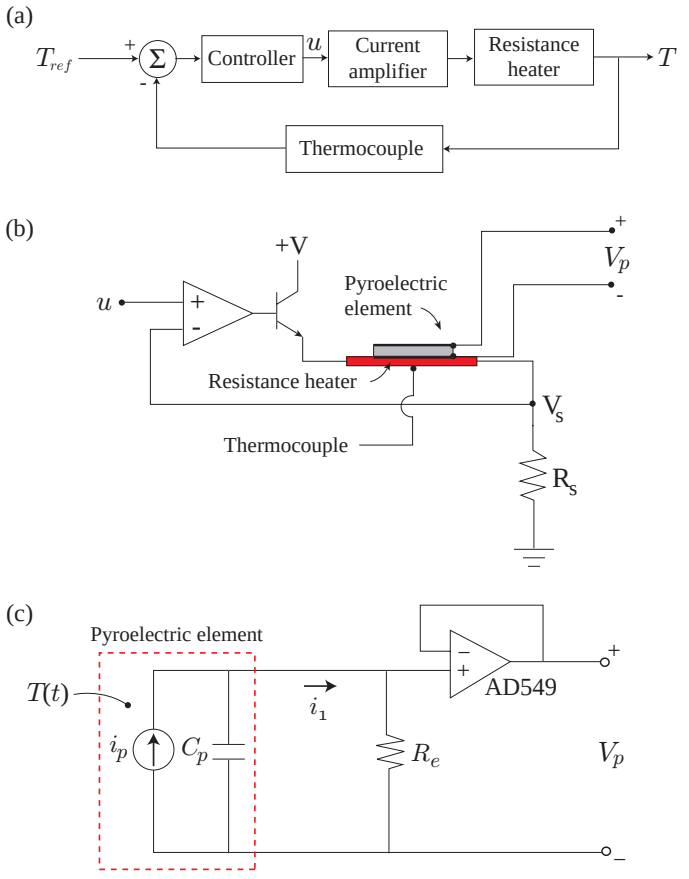

Figure 3. The experimental setup: (a) the block diagram of the temperature control system; (b) a schematic of the current amplifier, resistance heater, and thermocouple system; and (c) the circuit diagram for measuring generated power. The AD549 was used to isolate the experimental setup from measurement system.

The predicted peak power density for the PST and PMN-PT (assuming $p' = 416$ μCm^{-2}K^{-1}) materials were 0.60 μWcm^{-2} and 126.19 μWcm^{-2}. For the same surface area and temperature rate, the PST material improved the power density by nearly three orders of magnitude compared to the PZT-5A material.

Figure 5 shows the peak power density as a function of area and pyroelectric coefficient. The area was varied between 1.44 cm^2 (1.20 cm× 1.20 cm) to 3.63 cm^2 (1.91 cm× 1.91 cm) and the capacitance was adjusted accordingly by assuming a constant electrode separation for a parallel-plate capacitor model. The pyroelectric coefficient was varied between 238 and p'=6000 μCm^{-2}K^{-1}. The predicted result shows the potential for using thin-films with improved pyroelectric coefficient, as well as maximizing the area of the energy harvesting element.

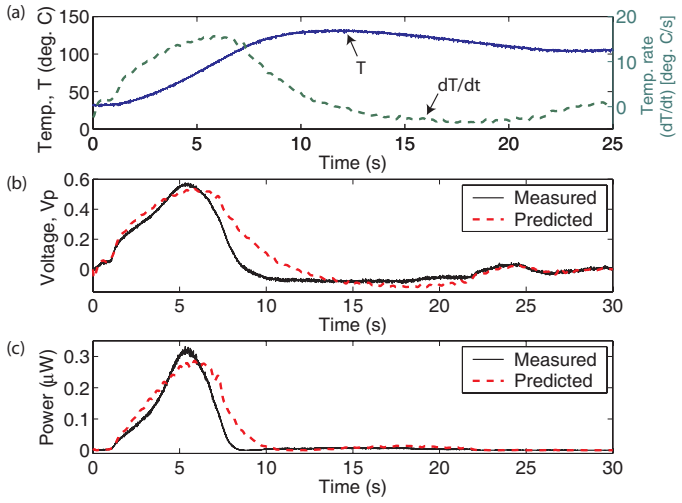

Figure 4. Measured and predicted results of power generated by PZT element. (a) Temperature and temperature rate (dT/dt) vs. time; (b) Measured and predicted PZT voltage vs. time; and (c) Measured and predicted power vs. time.

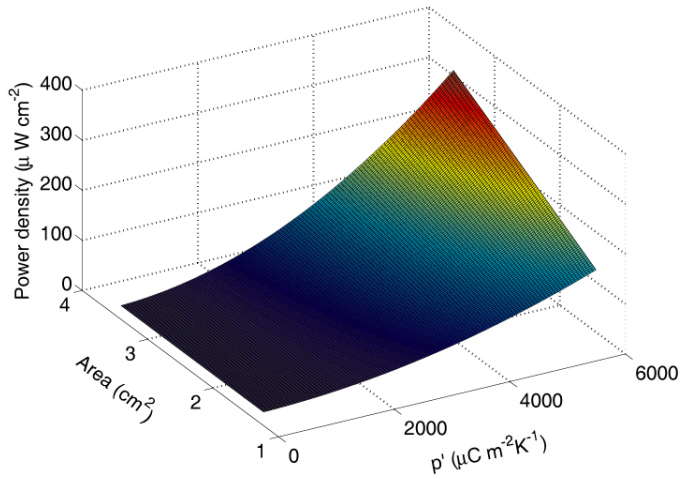

Figure 5. Predicted peak power density as a function of pyroelectric coefficient and area based on same boundary conditions as the experiment on PZT-5A.

5 CONCLUSIONS

The potential for energy harvesting via the pyroelectric effect was studied for a PZT-5A sample and a simple model was developed to predict the power generated. Measured and predicted results show good agreement and the measured peak power density was 0.23 μWcm^{-2} for approximately 15°Cs^{-1} temperature rate. Using the model, a thin-film with significantly higher pyroelectric coefficient showed nearly three orders of magnitude improvement in the peak power density under the same boundary conditions as the PZT-5A sample.

6 ACKNOWLEDGEMENTS

Authors would like to acknowledge the support of NextGen Aeronautics, specifically Shiv Joshi and Scott Bland, as well as the Air Force Research Laboratory. Authors also thank Andrew J. Fleming for making suggestions on the power measurement circuit.

REFERENCES

[1] Sodano, H. A., Inman, D. J., and Park, G., 2004. "A review of power harvesting from vibration using piezoelectric materials". *The Shock and Vibration Digest,* **36**(3), pp. 197 – 205.

[2] Roundy, S., Wright, P., and Rabaey, J., 2003. "A study of low level vibrations as a power source for wireless sensor nodes". *Computer Communications,* **26**(1), pp. 1131 – 1144.

[3] Paradiso, J. A., and Starner, T., 2005. "Energy scavenging for mobile and wireless electronics". *Prevasive Computing*, January - March, pp. 18 – 27.

[4] Nersessian, N., Carman, G. P., and Radousky, H. B., 2008. Energy havesting using a thermoelectric material.

[5] Sodano, H. A., Simmers, G. E., Dereux, R., and Inman, D. J., 2007. "Recharging batteries using energy harvested from thermal gradients". *Journal of Intelligent Material Systems and Structures,* **18**, pp. 3 – 10.

[6] Ujihara, M., Carman, G. P., and Lee, D. G., 2007. "Thermal energy harvesting device using ferromagnetic materials". *Applied Physics Letters,* **91**, p. 093508.

[7] Whatmore, R. W., 1986. "Pyroelectric devices and materials". *Rep. Prog. Phys.,* **49**, pp. 1335 – 1386.

[8] Borisenok, V. A., Koshelev, A. S., and Novitsky, E. Z., 1996. "Pyroelectric materials for converters of pulsed ionizing radiation energy into electric power". *Bulletin of the Russian Academy of Sciences, Physics,* **60**(10), pp. 1660 – 1662.

[9] Cuadras, A., Gasulla, M., Ghisla, A., and Ferrari, V., 2006. "Energy harvesting from PZT pyroelectric cells". In Intrumentation and Measurement Technology Conference, pp. 1688 – 1672.

[10] Bauer, S., 2006. "Piezo-, pyro- and ferroelectrets: soft transducer materials for electromechanical energy conversion". *IEEE Transactions on Dielectrics and Electrical Insulation,* **13**(5), pp. 953 – 962.

[11] Sebald, G., Lefeuvre, E., and Guyomar, D., 2008. "Pyroelectric energy conversion: optimization principles". *IEEE Trans. Ultrasonics, Ferroelectrics, and Frequency Cont.,* **55**(3), pp. 538 – 551.

[12] Lam, S. K., Wong, Y. W., Tai, L. S., Poon, Y. M., and Shin,

F. G., 2004. “Dielectric and pyroelectric properties of lead zirconate titanate/polyurethane composites”. *J. Appl. Phys.,* **96**(7), pp. 3896 – 3899.

[13] Watton, R., and Todd, M. A., 1991. “Induced pyroelectricity in sputtered lead scandium tantalate films and their merit for IR detector arrays”. *Ferroelectrics,* **118**, pp. 279 – 295.

[14] Todd, M. A., Donohue, P. P., Jones, J. C., Wallis, D. J., Slatter, M. J., Harper, M. A., and Watton, R., 1999. “Deposition and annealing of lead scandium tantalate thin films for high performance thermal detector arrays”. *Integrated Ferroelectrics,* **25**, pp. 113 – 123.

[15] Kumar, P., Sharma, S., Thakur, O. P., Prakash, C., and Goel, T. C., 2004. “Dielectric, piezoelectric and pyroelectric properties of PMN-PT (68:32) system”. *Ceramics International,* **30**, pp. 585 – 589.

[16] Huang, H., Sun, C. Q., Tianshu, Z., Hong, Z., Oh, J. T., and Hing, P., 2003. “Stress effect on the pyroelectric properties of lead titanate thin films”. *Integrated Ferroelectrics,* **51**, pp. 81 – 90.

[17] Mossi, K. M., Green, C., Ounaies, Z., and Hughes, E., 2005. “Harvesting energy using a thin unimorph prestressed bender: geometrical effects”. *J. of Intell. Mater. Syst. and Struct.,* **16**, pp. 249 – 261.